Colloids and Surfaces A: Physicochemical and Engineering Aspects 659 (2023) 130787

Contents lists available at ScienceDirect

Colloids and Surfaces A: Physicochemical and Engineering Aspects

journal homepage: www.elsevier.com/locate/colsurfa

Solid lipid nanoparticles and nanostructured lipid carriers of dual functionality at emulsion interfaces. Part II: active carrying/delivery functionality

Georgia I. Sakellari [a,*], Ioanna Zafeiri [a], Hannah Batchelor [b], Fotis Spyropoulos [a]

[a] School of Chemical Engineering, University of Birmingham, Edgbaston, Birmingham B15 2TT, UK
[b] Strathclyde Institute of Pharmacy and Biomedical Sciences, University of Strathclyde, 161 Cathedral Street, Glasgow G4 0RE, UK

HIGHLIGHTS

- Minimal loss of crystalline matter was observed for all systems over a storage period of 3 months.
- The degree of particle interfacial adsorption was calculated by deconvolution of DSC data.
- Active encapsulation did not affect the particle interfacial behaviour and Pickering functionality.
- Dual-functional Pickering SLNs and NLCs simultaneously regulated the release of curcumin.
- Long-term stability of the obtained release profiles was demonstrated.

GRAPHICAL ABSTRACT

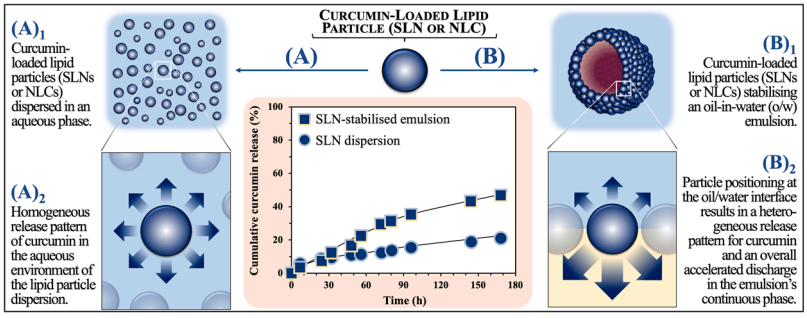

ARTICLE INFO

Keywords:
Solid lipid nanoparticles
Nanostructured lipid carriers
Pickering emulsion
Thermal stability
Mass transfer
Release performance

ABSTRACT

The utilisation of lipid nanostructures that can in tandem act as Pickering emulsion stabilisers and as active carrier/delivery systems, could potentially enable the development of liquid (emulsion-based) formulations with the capacity for multi-active encapsulation and delivery. Part I of this work focused on the first aspect of this two-fold functionality by investigating the capacity of both solid lipid nanoparticles (SLNs) and nanostructured lipid carriers (NLCs) to act as effective Pickering particles in o/w emulsions. Herein, attention shifts to the secondary functionality, with part II of this study assessing both SLNs and NLCs in terms of their capacity to act as carriers and release regulators for curcumin, a model hydrophobic active. The previously established Pickering functionality and physical properties in terms of particle size, zeta potential and interfacial tension of the lipid particles remained unaffected after encapsulation of curcumin. In emulsions, loss of crystalline (solid lipid) matter and particle interfacial presence were specifically investigated, as these aspects can impact upon the particles' active carrying and delivery performance. Low solid matter losses were recorded for all emulsions (ranging between 0% and 15%), with increasing liquid lipid fraction in the particles (SLNs to NLCs) resulting in relatively higher depletion of crystallinity. Removal of unadsorbed surfactant (remnant from the particle formation processing step) prior to emulsification led to higher particle interfacial occupancy. Despite said changes, the lipid particles' curcumin carrying capacity, expressed as encapsulation efficiency and loading capacity, did not differ between an emulsion and dispersion setting. Although the active carrying capacity was retained, it was

* Corresponding author.
E-mail address: gis823@bham.ac.uk (G.I. Sakellari).

https://doi.org/10.1016/j.colsurfa.2022.130787
Received 22 October 2022; Received in revised form 9 December 2022; Accepted 11 December 2022
Available online 12 December 2022

shown that the presence of the particles at the emulsion interfaces affects the curcumin release rate. Partial migration of curcumin to the oil droplet and creation of an additional release-inducing potential to the particles in close proximity to the droplet interface are proposed to be responsible for the overall faster active expulsion. What is more, the curcumin release profile from either SLNs or NLCs (also) stabilising an emulsion microstructure, was shown to persist after storage; either storage of the particles (up to 4 months) prior to emulsification, or storage of emulsions (up to 3 months) stabilised by 'freshly' formed lipid particles. Overall, the present study provides evidence that the two-fold functionality of the lipid particles can be indeed realised, markedly demonstrating that their concurrency does not compromise one another.

1. Introduction

Among the most desirable characteristics of an active carrying/delivery system is the ability to regulate the release of its encapsulated species, along with other physicochemical (e.g. surface properties, loading capacity) properties, tailoring of which can enable the development of targeted delivery systems (e.g. suitable for oral ingestion) [1–3]. Although approaches to manipulate these properties have been successfully devised for single active-carrying systems, additional challenges can be introduced once a secondary active is also encapsulated within the same formulation. These could relate to the need to independently control the kinetics of the release of each of the two entities, often via simple approaches, such as manipulating the formulation characteristics of the single microstructure carrying both. The development of formulations that allow the segregated/individual encapsulation of multiple actives could potentially address said challenges, as regulating the mode and rate of delivering each of the various species can be attempted by separately fine-tuning the properties of the sub-compartment (within the overall microstructure) where each is contained.

This strategy has already been explored using different formulation approaches, such as hierarchical multicompartmental triple emulsions [4], oil-in-water emulsion droplets stabilised by sodium caseinate/chitosan (protein/polysaccharide) co-precipitated complexes [5], and multicompartment polymeric hydrogels (composed of incompatible hydrocarbon and fluorocarbon nanoparticle cores) [6], among others. Pickering emulsions stabilised by solid lipid nanoparticles (SLNs) have recently emerged as a promising multicompartmental co-delivery system, that can facilitate the individually-tailored delivery of multiple encapsulated actives [7]. In this system, the lipid particles have the two-fold functionality of simultaneously stabilising the emulsion droplets, while also regulating the release of actives incorporated both within the particles and the emulsion droplets. Concerning the use of lipid particles as active delivery systems, nanostructured lipid carriers (NLCs) have also gained ground as carriers, due to the co-presence of a solid and liquid lipid (at room temperature) in their crystalline core creating imperfections, and thus allowing for higher active loadings [8,9]. Among the advantages that both types of lipid-based carriers (SLNs and NLCs) can offer are high loading capacities (for not only hydrophobic but also hydrophilic compounds), attained by selecting appropriate lipid matrix components [10–14], controllable release [15,16], and improved stability of the entrapped actives [17,18]. Therefore, understanding how (and to what extent) formulation parameters of both types of lipid particles (parameters which in part I of this study [19] were investigated for their effect on the Pickering stabilisation capacity of these lipid microstructures), affect their active carrying/delivery functionality, could eventually enable the attainment of a truly dual-functional system.

In emulsions, the regulation of mass transfer from the dispersed phase carrying the active to the external phase is typically achieved by modifying the interfacial layer architecture via the presence of a colloidal (or otherwise) load, which is what systems such as Pickering particles have been studied for in the past. A recent study revealed that the release rate of a model hydrophobic active (dimethyl phthalate) from o/w emulsions stabilised by emulsifiers with a Pickering-like characteristics, was hindered by the type of emulsifier chosen, and the permeability and thickness of the formed interfacial layer [20]. Exploiting the specific characteristics of lipid entities decorating an emulsion interface has been shown as a successful approach to achieve triggered release of encapsulated molecules. Frasch-Melnik et al. [21] and Garrec et al. [22] demonstrated that melting of the sintered fat shell formed at the surface of w/o droplets (shells consisting of monoglyceride and triglyceride crystals in the former, and monoglyceride and tripalmitin crystals in the latter study) led to complete release of the salt incorporated within the water droplets. Similarly, Dieng et al. [23] reported that SLNs can equally be used as release regulators of an active (ketoprofen) encapsulated within o/w emulsion droplets, employing a temperature-controlled mechanism.

However, challenges are introduced once an active is encapsulated within such lipid particles, which themselves are then positioned at an emulsion interface. On one hand it is still desirable to maintain the structural integrity of the layer formed by the particles at the interface, but on the other hand it is also endeavoured for the particles to sustain their active content and deliver it in a manner resembling the release behaviour exhibited in a non-emulsion scenario; i.e. release from an aqueous dispersion of the same particles. This is not a straightforward task, as there have been reports showing that solid lipid particle matter [24–26] and loaded active might both migrate into the dispersed oil phase, once particles are incorporated within an emulsion architecture. In terms of active transfer, Schröder et al. [27] simulated the diffusion of antioxidants (α-tocopherol and carnosic acid) incorporated within SLNs to the oil droplets over time using a fluorescent analogue (25-NBD cholesterol, 25-[N-[(7-nitro-2–1,3-benzoxadiazol-4-yl)methyl]amino]-27-norcholesterol), showing that there is a dynamic transfer of the lipophilic compounds to the droplets that occurs over short timescales. Milsmann et al. [28] employed a separated emulsion model system to suggest that a probe encapsulated within SLNs would show a prolonged release, caused by partitioning of said probe to the oil phase and o/w interface of the emulsions. However, the exact mechanism by which active migration into the droplets takes place in 'real' lipid particle-stabilised emulsion systems, as well as how formulation aspects of both SLNs and NLCs can be exploited to control such phenomena, have yet to be studied.

Part II of this work investigates whether adopting an active carrying and delivery functionality compromises the previously defined capacity of the lipid particles to act as Pickering emulsion stabilisers (part I), but also explores the parameters that affect this secondary (but concurrent) functionality and the mechanisms involved in its manifestation. An issue known to impact on the Pickering functionality of lipid particles, but in the present scenario potentially also their additional role as active carriers, is their capacity to preserve their solid matter once exposed to an emulsion setting [24–26]. Therefore, this study initially assesses how lipid particle type/composition (SLNs and NLCs of increasing solid-to-liquid lipid mass ratio) and interfacial occupancy can promote solid (fat) matter losses. Subsequently, the influence of curcumin (CRM, used as a model active) incorporation on the properties (including size, zeta potential and interfacial behaviour) of lipid particles "used-as-produced" (i.e., those containing excess surfactant, remnant from the particle formation stage) or "dialysed" (i.e., those essentially deprived of any such excess surfactant load), were explored. The ability of the now loaded-lipid particles to retain their Pickering stabilisation functionality

was then studied, and the droplet size and ζ-potential of the resulting systems were measured. Lastly, the release performance of (prior- and post-dialysis) lipid particles in an emulsion setting was investigated and compared to that observed in simple aqueous dispersions.

2. Materials and methods

2.1. Materials

Glyceryl behenate (Compritol® 888 ATO) was a kind gift from Gattefossé (Saint-Priest, France). Medium chain triglycerides (MCTs) (Miglyol® 812) were kindly provided from IOI Oleo (IOI Oleochemicals GmbH, Germany). Polyoxyethylene sorbitan monooleate (Tween® 80) and curcumin (≥65%, HPLC) were purchased from Sigma-Aldrich (Sigma-Aldrich, UK). Oxoid™ phosphate buffered saline (PBS) pH 7.4 tablets were obtained from Thermo Scientific (Sheffield, UK). Sunflower oil was purchased from a local supermarket, stored in a closed container at ambient temperature in the dark and used without any further purification. Double distilled water from Milli-Q systems (Millipore, Watford, UK) was employed throughout this study.

2.2. Lipid particle preparation

Lipid nanoparticle dispersions were fabricated using a melt-emulsification-ultrasonication method followed by cooling of solid and different solid-to-liquid lipid mass ratio (9:1, 8:2 and 7:3) lipid melts in an ice bath. When curcumin was loaded within the lipid particles, 0.5% w/w curcumin, in relation to the total lipid mass, was added to the lipid melt and kept under magnetic stirring until fully dissolved. All samples were stored at 4°C until further analysis. A detailed preparation protocol is given elsewhere [29]. The removal of excess unbound surfactant from the lipid dispersions was realised by immersing a known amount of each dispersion contained within cellulose dialysis membrane (43 mm width, 14 kDa M.W. cut-off, Sigma-Aldrich Company Ltd., Dorset, UK,) in distilled water under constant stirring at room temperature. The dialysis membranes were pre-hydrated in distilled water overnight. The dialysis medium was changed every 24 h and the process was continued until an equilibrium surface tension value (standard deviation of the last twenty measurements was smaller than 0.05 mN/m) similar to that of distilled water was obtained. Surface tension measurements were performed with a profile analysis tensiometer (PAT-1 M, Sinterface Technologies, Berlin, Germany). Briefly, a drop of the dissolution medium was suspended via a straight stainless-steel capillary (3 mm outer diameter) in air, with the cross-sectioned surface area remaining constant at 27 mm^2. Density values of the samples were determined using a densitometer (Densito, Mettler Toledo, US), at 20°C. Dialysed samples were retrieved from the tubing and diluted to their initial mass with distilled water, to maintain the initial lipid phase concentration at 2.5% w/w.

2.3. Emulsion preparation

The oil-in-water (o/w) emulsions were prepared with 90% (w/w) aqueous phase containing any of the different lipid nanoparticle systems (SLNs, NLCs) and 10% (w/w) sunflower oil phase. Emulsification was performed using a high intensity ultrasonic Vibra-cell™ VC 505 processor (Sonics & Materials, Inc., CT, USA), operating continuously at 750 Watt and 20 kHz, at a sonication amplitude of 95% of the total power over a period of 30 s. All samples were kept in an ice bath during processing, to avoid shear-induced heating. The produced systems were stored at 4°C until further analysis.

2.4. Particle/droplet size and ζ-potential measurements

The particle size expressed as *Z*-average and zeta potential (ζ-potential) of curcumin-loaded lipid nanoparticles used as produced and after dialysis were measured with dynamic light scattering (DLS) employing a Zetasizer Nano ZS (Malvern Instruments, UK). All measurements were performed at a backscattering angle of 173° at 25 °C, and samples were appropriately diluted to avoid multiple scattering phenomena. The refractive indices (RI) for the materials used were determined using a refractometer (J 357 series, Rudolph Research Analytical, USA) at 20 °C, and used accordingly [29]. For distilled water, the refractive index used was 1.33 and the absorption index was set at 0.01. Measurements were performed in triplicate and the average values with standard deviation (± S.D.) are presented. Laser diffraction (LD) was employed to determine the droplet size of the curcumin-loaded lipid particle-stabilised o/w emulsions after incorporation of curcumin in the lipid particles, using a Mastersizer 2000 (Malvern Instruments, UK) equipped with a Hydro SM manual small volume sample dispersion unit. The refractive index (RI) of sunflower oil was set at 1.47. All measurements were performed in triplicate. Zeta potential measurements of the o/w emulsion systems were performed following the method described above.

2.5. Interfacial tension measurements

Interfacial properties at the oil/water interface of the curcumin-loaded lipid nanoparticles used as produced and after removal of excess surfactant were determined with the pendant drop method utilising a profile analysis tensiometer (PAT-1 M, Sinterface Technologies, Berlin, German), at 20°C. A drop of the samples was suspended via a straight stainless-steel capillary (3 mm outer diameter) in the sunflower oil phase contained in a quartz cuvette, with the cross-sectioned surface area remaining constant at 27 mm^2. Data were collected until equilibrium was reached (standard deviation of the last twenty measurements was smaller than 0.05 mN/m). Density values of the samples were determined using a densitometer (Densito, Mettler Toledo, US), at 20°C. All measurements were conducted in at least triplicate.

2.6. Thermal analysis

The thermal behaviour of the lipid particles both in the dispersions and within the emulsion systems was assessed via Differential Scanning Calorimetry (DSC) using a Setaram μDSC3 evo microcalorimeter (Setaram Instrumentation, France). The temperature was cycled between 20 and 80°C at a heating rate of 1.2 °C/min. Data processing, including information about peak temperatures, melting enthalpies and deconvolution of peaks, was carried out using the Calisto Processing software (Setaram Instrumentation, France). Information from the thermal profiles of the lipid particles within this temperature range was used to study the behaviour of the particles within an emulsion setting and assess their stability over time (immediately and at 4, 8 and 12 weeks after emulsification). More specifically, the loss of crystalline matter was determined using information from the total melting enthalpies of the particles within an emulsion environment (ΔH_{em}^{T}) and those in an aqueous dispersion setting (ΔH_{dis}), and was expressed as a $\Delta H_{em}^{T}/\Delta H_{dis}$ ratio. The ΔH_{dis} and ΔH_{em}^{T} values were obtained from peak integration of the particle dispersion and particle-stabilised emulsion melting thermograms, respectively. The proportion of lost particles was calculated as a fraction of the particles initially present in the aqueous dispersions ((ΔH_{dis} - ΔH_{em}^{T})/ΔH_{dis}). Information regarding the relative positioning of the lipid particles remaining within the emulsion systems was gained through deconvolution of the two melting events (ΔH_{em}^{i}, $i =$ 1 or 2) occurring in each system. Particles were distinguished into two categories; particles present in the continuous phase (denoted as ΔH_{em}^{1} and peak 1) or at the emulsion interface (denoted as ΔH_{em}^{2} and peak 2). The proportion of each population was calculated as a fraction and expressed as unadsorbed ($\Delta H_{em}^{1}/(\Delta H_{em}^{1} + \Delta H_{em}^{2})$) and adsorbed ($\Delta H_{em}^{2}/(\Delta H_{em}^{1} + \Delta H_{em}^{2})$) particles. Examples of the peak integration/deconvolution of representative lipid particle dispersion samples and their respective emulsion systems are provided in Supplementary Information (Fig. S1). All enthalpy values and thermograms reported, are normalised

for the amount of crystallising material present in each sample. Specifically for the emulsion systems, each thermogram was normalised using the information of the respective SLN or NLC dispersion (Fig. S2) that was used for the emulsification. All measurements were performed at least in triplicate and on three independently prepared samples.

2.7. Imaging

Representative images of the microstructure of o/w emulsion droplets stabilised with curcumin-loaded lipid particles were obtained using confocal laser scanning microscopy (CLSM) (Leica TCS SPE, Heidelberg, Germany), equipped with a laser operating at a wavelength of 532 nm. The excitation wavelength for curcumin was set at 488 nm and the images were acquired with a 63x oil immersion lens using a coverslip to cover the sample. Emulsion systems with larger droplet sizes were visualised by preparing the samples with a low level of shear, employing a high-shear mixer (Silverson L5 M, Silverson Machines Ltd, UK), operating at 9000 rpm for 2 min

2.8. Encapsulation efficiency and loading capacity

The encapsulation efficiency (EE) and loading capacity (LC) of the curcumin-loaded lipid dispersions and curcumin-loaded particle-stabilised emulsions was determined by ultrafiltration using centrifugal ultrafiltration tubes (Amicon® Ultra-4 filter 10 kDa cut-off, Millipore, Billerica, MA, USA). 1 mL of the samples was added to the upper chamber of the centrifugal tube and centrifuged at 2400 rcf for 1 h at room temperature using a SIGMA 3 K-30 centrifuge (SciQuip®, UK). The concentration of unentrapped curcumin in the filtrate was subsequently determined by measuring the UV absorbance (Genova Bio Life Science Spectrophotometer, Jenway®, Cole-Palmer, UK) at 425 nm, using a calibration curve that has been previously generated with linearity studied for 0–6 μg/mL and linear regression value of $R^2 = 0.9995$. The EE was calculated using the following equation:

$$EE = \frac{W_{i.CRM} - W_{u.CRM}}{W_{i.CRM}} \times 100(\%) \quad (1)$$

$$LC = \frac{W_{i.CRM} - W_{u.CRM}}{W_{l.p.}} \times 100(\%) \quad (2)$$

where $W_{i.\ CRM}$ is the amount of curcumin that was initially used during the preparation of the aqueous lipid dispersions and $W_{u.\ CRM}$ is the amount of curcumin measured in the filtrate, and $W_{l.p.}$ is the total amount of the lipid components used in the dispersions.

2.9. In vitro release

In vitro release of curcumin, used as a model hydrophobic active, from curcumin-loaded lipid particle dispersions alone and particle-stabilised (Pickering) o/w emulsions was performed by diffusion through a dialysis membrane. A known amount of the particle dispersions or the Pickering emulsions was enclosed in a cellulose dialysis membrane (43 mm width, 14 kDa M.W. cut-off, Sigma-Aldrich Company Ltd., Dorset, UK), and the tubing was introduced in the in vitro release medium (130 g) consisting of phosphate buffer saline (PBS, pH 7.4) and 1.0% w/w Tween® 80. The specific type and mass of dissolution medium were chosen to enable sufficient curcumin solubilisation and ensure sink conditions (the active concentration was approximately eight times less than its saturation solubility in the dissolution medium). A pure curcumin solution was prepared by dissolving equal amount of curcumin to that in the lipid particle dispersions (0.0125% w/w) in a solution that consisted of the dissolution medium. Dialysis membranes were soaked in the dissolution medium overnight, prior to usage. At predetermined time intervals, 1 mL aliquots of the dissolution medium were collected and analysed by UV-Vis spectrophotometry (Genova Bio Life Science Spectrophotometer, Jenway®, Cole-Palmer, UK), at 425 nm using a calibration curve that has been previously generated with linearity studied for 0–6 μg/mL and linear regression value of $R^2 = 0.9995$. To maintain sink conditions, the sampled dissolution medium was each time replaced by an equal volume of fresh media. The release profiles were studied using an Incu-Shake MIDI shaker incubator (Sciquip, UK) operating at 25°C under constant shaking (180 rpm). For stability assessments, the lipid particle dispersions were used/studied immediately after preparation and after 4 months of storage, and their respective particle-stabilised emulsions were assessed immediately after emulsification and after 3 months of storage at 4°C. Each test was conducted in triplicate using independently prepared samples.

2.10. Modelling of release data

The release data from the lipid particles and the particle-stabilised emulsions were fitted into the mechanistic model described by Crank [30], to gain further insight regarding the underlying release mechanism. The diffusion coefficient (D) was determined as follows:

$$\frac{Q_t}{Q_\infty} = 1 - \frac{6}{\pi^2}\sum_{n=1}^{\infty}\frac{1}{n^2}\exp\left(-\frac{Dn^2\pi^2 t}{r^2}\right) \quad (3)$$

where Q_t is the mass of active released at time t, Q_∞ is the total mass of active released when the formulation is exhausted, n is a dummy variable, r is the particle radius, and D is the apparent diffusion coefficient of the active within the system. The diffusion coefficients (D) and the coefficient of determination (R^2) used as a model fitness indicator are given in Table 2.

2.11. Statistical analysis

Samples were analysed in at least triplicate and averages are reported with standard deviation (± S.D.). Figures depict the calculated average with error bars showing the standard deviation above and below the average. Comparison of means was conducted by ANOVA analysis followed by an all pairwise multiple comparison test using the Student-Newman-Keuls Method (SigmaPlot 14.5). The differences were considered statistically significant when $p < 0.05$.

3. Results and discussion

3.1. The role of particle integrity and positioning in an emulsion setting

Literature suggests that in an emulsion setting, the presence of an oil phase can provoke the dissolution of solid matter from lipid particles positioned at the interface; e.g. dissolution into the dispersed phase oil droplets in the case of o/w emulsions [24–26]. Such a decline in solid/crystalline matter could thus lead to loss of the lipid particles' Pickering functionality, and also jeopardise the particles' active carrying capacity. Parameters that could affect the occurrence and/or kinetics of such phenomena, include the lipid particles' formulation characteristics and the presence of additional (unadsorbed) surfactant in the continuous phase of the Pickering emulsions. Therefore, SLNs and NLCs with increasing liquid lipid content (10%, 20% and 30% w/w) used as produced and after removal of excess surfactant from their aqueous dispersion phase, were used as Pickering stabilisers and investigated for their water/oil interfacial presence, a parameter that could also potentially affect their active carrying/delivery capacity.

3.1.1. Loss of particle crystalline matter within emulsion systems

In this study, information regarding the loss of crystalline matter was gained through the melting thermograms of the emulsions, and specifically the ratio between the total melting enthalpies of the particles within an emulsion environment (ΔH_{em}^{T}) and those in a lipid particle aqueous dispersion setting (ΔH_{dis}) [24]. These ratios were calculated

according to the melting events occurring in each system immediately after preparation (Fig. 1), and the resulting enthalpy ratios themselves are presented in Fig. 2. Enthalpy data for all systems (particle-stabilised o/w emulsions or particle aqueous dispersions) were normalised against the mass of solid/crystalline matter present in each system, as in both cases the solid lipid is the only component undergoing phase transition. Herein, the impact of the oil addition was explicitly studied, as any effects arising from the liquid lipid incorporation in the solid matrix have already been investigated [29] and accounted for during enthalpy normalisation. Based on the calculated ratios, it is evident that the loss of solid lipid matter was minimal for all systems used as produced and after dialysis, with the percentage of original crystalline matter (generated at the particle manufacture stage) remaining in the systems following oil introduction (emulsification) ranging between 85% and 100%. Zafeiri et al. [24] investigated the dissolution of solid material from SLNs in increasing fractions of sunflower o/w emulsions, using cetyl palmitate and tristearin particles (2.5% w/w) fabricated in the presence of Tween® 80 or sodium caseinate (0.8% w/w). It was shown that sodium caseinate provided improved shielding over mass transfer phenomena compared to Tween® 80 (95 versus 68% of solid lipid matter was found to persist after emulsification for the 10% oil phase o/w emulsions, respectively), and cetyl palmitate exhibited greater loss of crystalline content (in the range of 55% and 75%) compared to tristearin (between 5% and 10%). Overall, it was suggested that dissolution mainly occurs shortly after emulsification, and the importance of the type and concentration of surfactant, and the type of lipid source used, relative to the rate of oil exchange was underlined. These observations have also been highlighted in a number of studies exploring the rate of oil exchange between o/w emulsion droplets and an aqueous phase, with surfactant molecules/micelles facilitating the transfer [26,31–34]. Notably, Samtlebe et al. [26] proposed that in emulsions containing SLNs fabricated with a relatively high aqueous solubility solid lipid, emulsion-originating oil molecules solubilised in micelles, diffuse and dissolve in the crystalline fat, thus promoting increased lipid mass transfer. Herein, the presence of medium chain triglyceride molecules (Miglyol® 812) in the NLCs appears to have induced solid lipid mass transfer, particularly in the case of the 8:2 and 7:3 NLCs, compared to the SLN- and 9:1 NLC-containing formulations; suggested by the statistically significant changes in the $\Delta H^T_{em}/\Delta H_{dis}$ ratios (Fig. 2). Part I of this study [19] demonstrated, that increasing the liquid lipid content of the

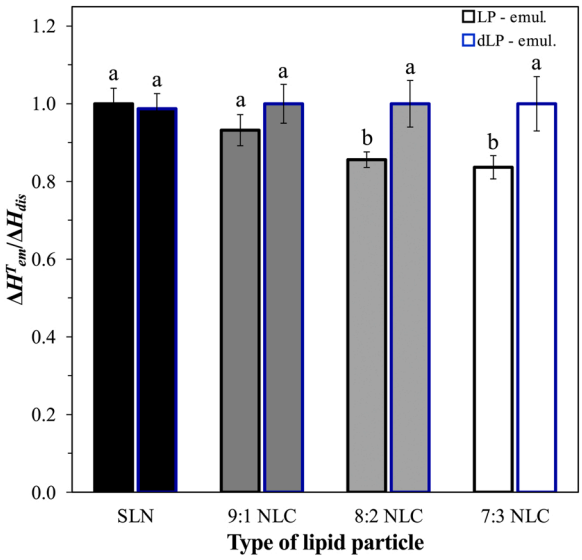

Fig. 2. Ratio of total melting enthalpies of the particles within an emulsion environment and those in a lipid particle dispersion setting ($\Delta H^T_{em}/\Delta H_{dis}$), representing the amount of crystalline material remaining within the emulsions stabilised by different types of lipid particles. The particles were either used as produced (LP), or after removal of excess surfactant (dLP). Identical lowercase letters indicate no significant differences between samples (for $p < 0.05$ and sample size equal to 3).

NLCs renders them more hydrophilic. Hence, it could be postulated here, that the increased hydrophilicity of the 8:2 and 7:2 NLC lipid matrix, further provoked oil dissolution and diffusion phenomena. When it comes to emulsions fabricated with lipid particles used after dialysis, the absence of excess surfactant (possibly in the form of micelles) from the continuous phase led to depletion in the loss of crystalline matter. This is more evident for the highest liquid lipid content particles (8:2 and 7:3 NLCs), possibly due to their already lower $\Delta H^T_{em}/\Delta H_{dis}$ ratios.

It was previously shown [19], based on the melting and crystallisation thermograms of the lipid particle dispersions, that removal of excess surfactant via dialysis did not alter their thermal behaviour. Glyceryl behenate SLNs displayed a level of polymorphism with a minor

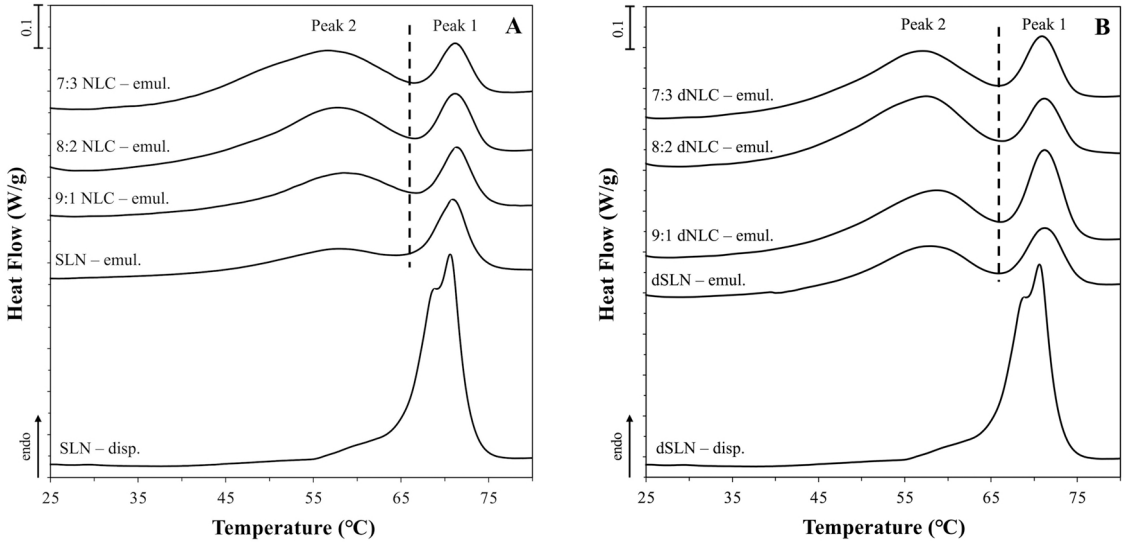

Fig. 1. DSC melting thermograms of particle-stabilised o/w emulsion prepared with different types of lipid particles (SLN, 9:1 NLC, 8:2 NLC and 7:3 NLC) before (A) and after removal of excess surfactant (B) from the aqueous lipid particle dispersions. The thermograms of the SLN formulation before and after dialysis are included in the corresponding graphs for comparison purposes. The curves were normalised for the amount of solid matter present in each sample and shifted along the ordinate for better visualisation. The dashed lines are used to distinguish between different thermal events.

shoulder (at 69.2°C) appearing on the main melting event at 70.7°C (also visible here in Fig. 1), that was shown to progressively intensify as the MCT (liquid lipid) content (9:1, 8:2 and 7:3 solid-to-liquid lipid mass ratios) in the NLCs increases (Fig. S2) [29]. Introduction of sunflower oil (emulsification) led to broadening of the main peak and appearance of a secondary peak at lower temperatures (~57°C), the intensity of which increased with increasing liquid lipid concentration in the lipid particle composition (Fig. 1*A & B*). This phenomenon has also been described in other studies employing lipid particles as Pickering emulsion stabilisers, and it was proposed that the partition in the melting profile of the solid lipid was caused by the relative location of the particles in the system; either particles remaining unadsorbed in the continuous phase (peak at higher temperature, herein denoted as peak 1), or particles adsorbed at the interface of the emulsion droplets (peak at lower temperature, denoted as peak 2 in this study) [27,35,36]. More specifically, it has been shown that the type of lipid [35], the emulsion fabrication process (addition of particles prior- or post-homogenisation) [27], and the addition and type of surfactant [36], are among the factors affecting the relative intensity of the two peaks. Although a clear explanation regarding the difference in the melting temperatures of the adsorbed and unadsorbed particles has not been proposed, it could be assumed that the diversity in the specific heat capacities between the surrounding phases (sunflower oil and water, respectively) contributes to the way that heat transfers to the solid lipid matter during melting, with the oil phase heating up faster due to the lower specific heat capacity [37]. Overall, all types of particles retained a high proportion of their original solid lipid content, a parameter that could potentially alter their ability to preserve their active carrying capacity and delivery in a sustainable manner.

3.1.2. *Lipid particle type and its effect on the SLN/NLC interfacial presence*

Another facet of the lipid particles' capacity to maintain their active carrying/delivery functionality is their relative positioning within the emulsion microstructure. Although it has been already established that the largest proportion of crystalline matter is maintained after emulsification, in such dynamic systems, the close proximity of the particles with the droplet interface could potentially affect their capacity to regulate the delivery of the enclosed active. Information about the proportion of lipid particles either present at the emulsion interface (i.e. exposed to the oil content in the droplets) or in the continuous phase (i.e. only largely exposed to an aqueous environment), could assist in discerning any such contributions on the overall active carrying/delivery performance of these systems.

To gain further insight regarding the distribution of lipid particles remaining in the emulsion systems, the melting curves of all lipid particle-stabilised emulsions were deconvoluted into two individual peaks; see Fig. 1*A & B*. This was performed for both different types of lipid particles (SLNs and NLCs), and for particles used before and after dialysis, as removal of excess surfactant could potentially affect their interfacial residency. The corresponding melting enthalpy for each peak was then calculated and the resulting ratios were determined (see *Section 2.6*) to distinguish between the fraction of adsorbed and unadsorbed particles within the emulsion systems. As depicted in Fig. 3 *(top)*, the proportion of lipid particles residing at the emulsion interface is approximately 60% (of the total population of remnant particles) and remains similar for both SLNs and NLCs. For lipid particles used after removal of excess surfactant, although the values were similar for different solid-to-liquid lipid mass ratios, they appear to be slightly higher than that of particles used as produced. Absence of free surfactant from the continuous phase could potentially allow a higher proportion of particles to reside at the interface of the droplets compared to the emulsions fabricated with the 'as produced' particle dispersions, where it could be assumed that part of the droplet interface is occupied by surfactant molecules. On the contrary, the ratio of unadsorbed particles (in the range of 30%) decreases with increasing amount of MCTs (Fig. 3, *bottom*) in both cases. This is particularly obvious for the two particle

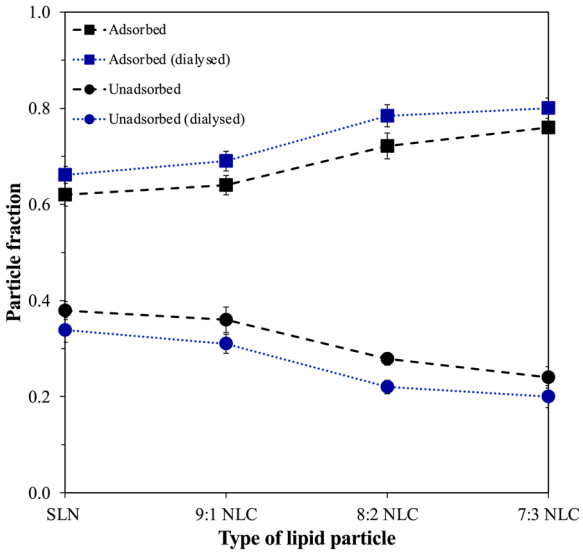

Fig. 3. Fraction of lipid particles unadsorbed and adsorbed for the different types of lipid particles used before and after dialysis, within an emulsion setting. For the ΔH^{i}_{em} calculations, the peaks were defined following deconvolution of the peaks presented in Fig. 1. When not visible, error bars are smaller than symbols.

formulations with the highest liquid lipid content (8:2 and 7:3 NLCs). To begin with, this observation needs to be approached cautiously, as the peaks ascribed to adsorbed particles (peak 2) for these two systems could also encompass the melting of polymorphic forms present in both adsorbed and unadsorbed particles (Fig. S2). The presence of non-spherical particles as suggested by the different polymorphs, particularly in the DSC thermograms of the 8:2 and 7:3 NLC dispersions [19,29], could suggest different packing/arrangement at the emulsion interface [38,39]. Additionally, the smaller particle size and differences in the zeta potential values of the aforementioned formulations (even though at marginal level) [29] could further support the requirement for higher interfacial residency. Such phenomena, not only explain the trends observed for the unadsorbed particles, but also for the respective adsorbed particles in the same formulations (Fig. 3, *top*). Another possible explanation when it comes to the decreasing percentage of unadsorbed particles in the systems with used as produced particles could be found in the occurrence of particle replacement at the emulsion interface. As more crystalline matter is lost at the emulsion interface, which is also reflected in the concurrent increase of lost particles (Table 1), the proportion of particles moving from the continuous phase to substitute the matter lost and maintain the same surface coverage increases (Fig. 4). This is in agreement with findings previously reported in literature [40], where it is shown that particles are reversibly adsorbed onto the emulsion droplets, and exchanges can occur between the continuous phase and the droplet interface. The data acquired from the DSC spectra shown here appear to give lower particle interfacial occupancy values when compared to the theoretical values of the (maximum) proportion of unadsorbed particles reported in part I of this work [19]. This suggests an overestimation in the latter theoretical values that could be attributed to 'adsorbed particle'-'free particle' bridging, that has previously been reported for particles covered by thin surfactant layers [41,42], or simply by the formation of multilayers of particles around the emulsion droplets (rather than the single layer assumed in the theoretical calculation). Information gained here does not only contribute to understanding regarding the effect of certain formulation parameters on the water/oil interfacial presence of the particles, but it could also assist in elucidating the active regulation mechanism of the particles in relation to their relative interfacial location within the emulsion systems in a later step.

Table 1
ΔH_{dis}, ΔH^{T}_{em}, ΔH^{i}_{em}, and T^{i}_{melt} of o/w emulsions stabilised by different SLN and NLC (9:1, 8:2 and 7:3) dispersions used as produced and after dialysis and measured at various time intervals over a storage period of 12 weeks at 4 °C. For the ΔH^{i}_{em} calculation, the peak separation was performed according to the peaks presented in Fig. 1, with peak 1 corresponding to unadsorbed and peak 2 to adsorbed particles. The fraction of particles lost overtime is also included for comparison purposes.

Type of lipid particle	Storage period (weeks)	ΔH_{dis} (J/g)	ΔH^{T}_{em} (J/g)	ΔH^{i}_{em} (J/g)		T^{i}_{melt} (°C)		Lost particles fraction
				ΔH^{1}_{em}	ΔH^{2}_{em}	T^{1}_{melt}	T^{2}_{melt}	
SLN	0	150.2 ± 2.3	148.0 ± 4.2	88.3 ± 4.0	55.6 ± 7.2	57.9 ± 1.1	71.0 ± 0.2	0.0 ± 0.0
	4	146.8 ± 2.2	145.8 ± 8.4	92.4 ± 3.8	53.2 ± 8.4	59.4 ± 0.9	71.7 ± 0.3	0.0 ± 0.0
	8	145.6 ± 6.7	144.7 ± 8.2	94.6 ± 4.7	53.1 ± 9.1	58.4 ± 0.7	71.0 ± 0.5	0.0 ± 0.0
	12	140.9 ± 5.4	140.8 ± 6.2	90.6 ± 5.8	47.3 ± 6.3	58.9 ± 0.5	71.1 ± 0.3	0.1 ± 0.0
9:1 NLC	0	146.1 ± 4.1	136.2 ± 4.4	85.3 ± 5.7	47.8 ± 7.7	58.5 ± 0.8	71.3 ± 0.2	0.1 ± 0.0
	4	141.7 ± 2.7	137.8 ± 3.1	91.5 ± 7.5	44.4 ± 4.3	59.5 ± 0.6	71.4 ± 0.1	0.1 ± 0.0
	8	143.1 ± 6.5	142.8 ± 9.9	94.5 ± 5.4	44.7 ± 6.7	58.9 ± 0.3	71.4 ± 0.1	0.1 ± 0.0
	12	147.7 ± 3.8	143.3 ± 4.7	95.9 ± 1.9	43.2 ± 6.0	59.1 ± 0.4	71.3 ± 0.2	0.1 ± 0.0
8:2 NLC	0	148.4 ± 3.2	128.0 ± 2.7	93.6 ± 2.5	36.4 ± 1.0	58.0 ± 0.3	71.2 ± 0.1	0.1 ± 0.0
	4	145.9 ± 6.3	136.5 ± 8.1	101.0 ± 10.5	35.5 ± 3.7	58.0 ± 0.3	71.5 ± 0.2	0.1 ± 0.0
	8	138.2 ± 2.9	135.9 ± 3.6	101.9 ± 2.8	34.0 ± 1.6	58.2 ± 0.2	71.4 ± 0.3	0.1 ± 0.0
	12	134.0 ± 4.7	127.1 ± 6.9	92.6 ± 1.0	32.5 ± 1.5	58.4 ± 0.1	71.5 ± 0.2	0.1 ± 0.0
7:3 NLC	0	144.9 ± 5.0	121.2 ± 3.7	93.4 ± 7.1	27.8 ± 2.7	55.9 ± 3.4	71.4 ± 0.5	0.1 ± 0.0
	4	142.7 ± 2.6	133.6 ± 10.3	102.5 ± 5.4	29.2 ± 5.9	57.7 ± 1.5	71.2 ± 0.3	0.1 ± 0.0
	8	141.2 ± 3.4	134.7 ± 14.5	105.9 ± 8.4	28.8 ± 6.6	56.9 ± 0.9	71.3 ± 0.2	0.1 ± 0.0
	12	135.4 ± 5.3	130.8 ± 13.2	98.7 ± 6.1	32.1 ± 9.2	57.1 ± 1.1	71.4 ± 0.1	0.1 ± 0.0
dSLN	0	145.0 ± 5.1	143.9 ± 5.8	95.6 ± 4.2	50.2 ± 5.7	57.9 ± 1.1	71.0 ± 0.2	0.0 ± 0.0
	4	148.9 ± 3.5	148.2 ± 7.6	94.5 ± 2.7	51.7 ± 8.9	58.2 ± 0.8	71.8 ± 0.2	0.0 ± 0.0
	8	147.5 ± 6.1	146.3 ± 10.5	93.2 ± 3.2	51.1 ± 7.4	58.1 ± 0.6	71.4 ± 0.1	0.0 ± 0.0
	12	148.9 ± 3.8	146.6 ± 8.9	99.4 ± 6.1	54.2 ± 13.2	58.0 ± 0.7	71.2 ± 0.3	0.0 ± 0.0
9:1 dNLC	0	149.9 ± 4.7	149.5 ± 14.3	106.7 ± 5.9	45.2 ± 6.9	58.5 ± 0.8	71.3 ± 0.2	0.0 ± 0.0
	4	144.9 ± 2.6	141.0 ± 12.6	108.0 ± 8.8	41.0 ± 12.8	57.9 ± 0.5	71.3 ± 0.1	0.0 ± 0.0
	8	148.1 ± 4.6	146.1 ± 10.4	107.3 ± 5.9	43.3 ± 12.5	57.8 ± 0.4	71.2 ± 0.2	0.0 ± 0.0
	12	150.9 ± 5.1	147.5 ± 12.4	104.6 ± 4.5	48.2 ± 12.4	58.1 ± 0.2	71.4 ± 0.1	0.0 ± 0.0
8:2 dNLC	0	138.7 ± 4.1	137.3 ± 9.4	108.2 ± 5.4	31.1 ± 2.7	58.4 ± 1.8	71.2 ± 0.4	0.0 ± 0.0
	4	140.9 ± 3.4	140.2 ± 11.3	115.6 ± 7.6	33.9 ± 0.7	58.3 ± 0.9	71.2 ± 0.1	0.1 ± 0.0
	8	141.7 ± 3.3	140.3 ± 10.6	109.1 ± 6.3	33.0 ± 5.2	58.1 ± 0.4	71.0 ± 0.2	0.0 ± 0.0
	12	137.7 ± 4.7	135.4 ± 9.3	113.2 ± 4.1	32.2 ± 8.6	58.1 ± 0.3	71.3 ± 0.2	0.0 ± 0.0
7:3 dNLC	0	139.0 ± 11.1	138.8 ± 3.5	109.3 ± 5.4	29.3 ± 3.7	55.9 ± 3.4	71.4 ± 0.5	0.0 ± 0.0
	4	135.6 ± 5.9	132.2 ± 4.4	108.7 ± 8.9	32.3 ± 4.7	57.2 ± 2.9	71.5 ± 0.3	0.1 ± 0.0
	8	136.2 ± 5.1	131.6 ± 3.8	107.6 ± 6.4	31.8 ± 2.8	56.9 ± 1.1	71.1 ± 0.3	0.0 ± 0.0
	12	140.6 ± 4.3	139.4 ± 7.9	106.3 ± 5.6	35.8 ± 3.4	57.1 ± 1.5	71.2 ± 0.2	0.0 ± 0.0

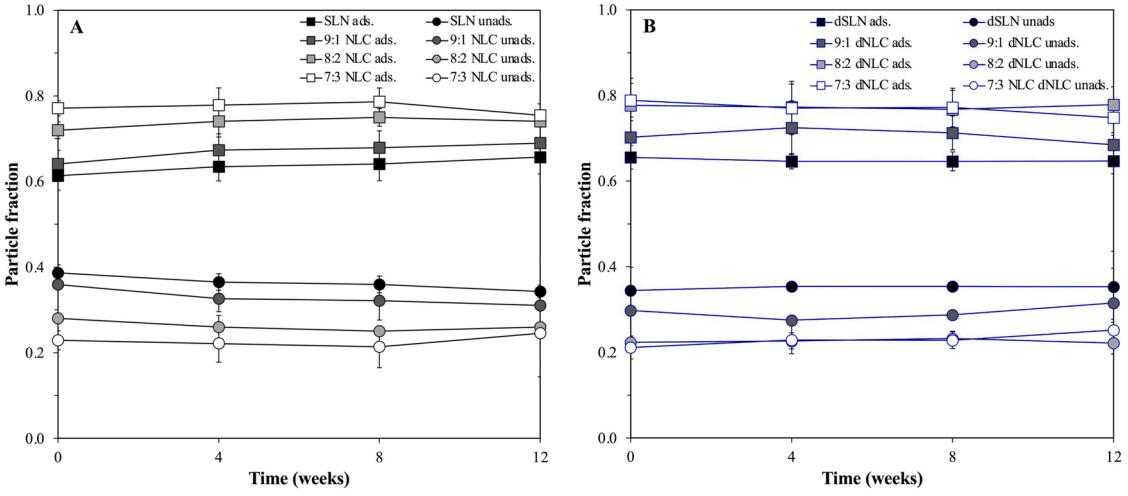

Fig. 4. Time evolution of the proportion of lipid particles adsorbed and unadsorbed for the different types of lipid particles used as produced (A) and after dialysis (B), within emulsion systems.

3.2. Effect of active incorporation on the lipid particle Pickering functionality

3.2.1. Size, zeta potential and interfacial properties of lipid particles

Prior to studying the active carrying/delivery capacity of curcumin-loaded particles within an emulsion setting, the effect of curcumin encapsulation on the size, ζ-potential and dynamic interfacial tension reduction ability of the SLN and 7:3 NLC formulations (used as produced or after dialysis) was studied. The choice of these two formulations was based on the fact that they represent the two extremes in terms of liquid lipid particle composition investigated here. Regarding the particle size, a slight *Z*-average increase was observed after the addition of curcumin in the two types of lipid particles (Fig. 5*A*), that has also been previously identified and attributed to lipid core swelling due to the presence of the active [29]. The effect that the removal of excess surfactant (via dialysis) has on (CRM-loaded) particle size was the same as that previously observed for 'blank' lipid particles [19], with a statistically significant increase only shown for the 7:3 NLCs. Similarly, no further changes after

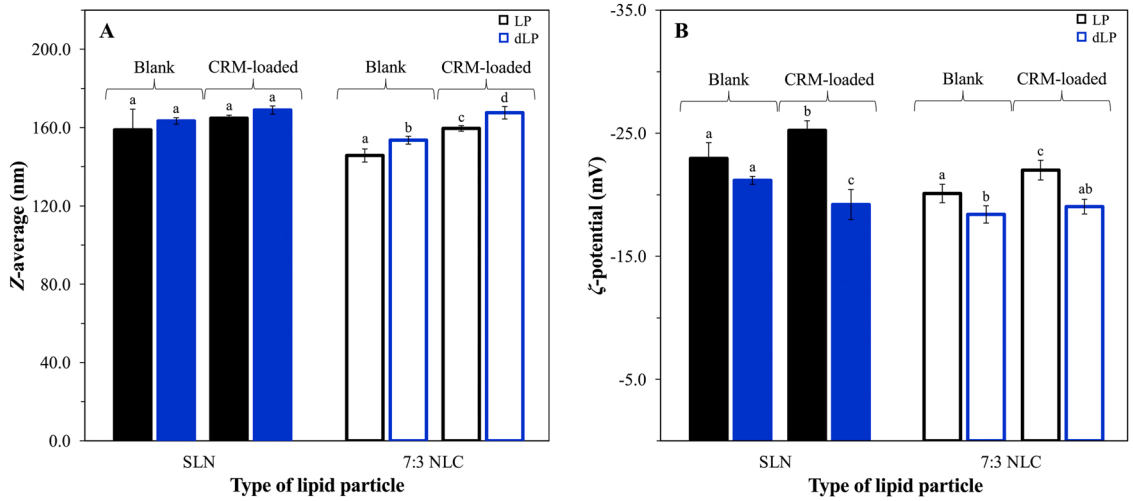

Fig. 5. Particle size (Z-average) (A) and ζ-potential (B) of curcumin-loaded lipid particle dispersions before (CRM-loaded LP) and after dialysis (CRM-loaded dLP). The respective data for blank lipid particles are also presented for comparison purposes. Identical lowercase letters indicate no significant differences between samples (for $p < 0.05$ and sample size equal to 3).

curcumin entrapment were recorded for the ζ-potential values and interfacial tension reduction capacity of both lipid particle dispersion types (either used as produced or after dialysis), apart from those already described for the respective blank formulations (Fig. 5B & 6, respectively). A more in-depth discussion of said differences can be found in part I of this work [19].

3.2.2. *Emulsion stabilisation behaviour*

Having established that the encapsulation of curcumin does not alter characteristics of the lipid particles that were previously shown to contribute to effective Pickering emulsion functionality, the curcumin-loaded SLN and 7:3 NLC formulations were indeed used to stabilise o/w emulsions and the droplet size and ζ-potential of the resulting systems were measured (Fig. 7*A & B*). As depicted in Fig. 7*A*, both (SLN- or NLC-stabilised) Pickering o/w emulsions fabricated using lipid particle dispersions where excess surfactant had been removed (dialysed), showed an additional droplet size population at larger sizes compared to the ones prepared with dispersions before dialysis. This is in agreement with what was observed for blank lipid particle-stabilised emulsions (*inset graph,* Fig. 7*Ai*) [19]. Possible explanations could lie in the interfacial tension reduction capacity differences between the dispersions (with dialysed particles having higher interfacial tension equilibrium values), lack of excess surfactant in the continuous phase and/or reduced wettability by the aqueous phase for the dialysed particles [43,44]. Correspondingly, the ζ-potential values demonstrated the same trends as for the blank systems, with no further changes caused due to the presence of the active (Fig. 7*B*). Finally, the Pickering stabilisation in the presence of curcumin for a representative system (CRM-dSLN-stabilised emulsion) was confirmed using CLSM (inset, Fig. 7*Aii*). The work presented here suggests that lipid particle microstructural design for Pickering performance can precede the development of active encapsulation strategies. Thus, as long as the latter do not impact on key indicators of Pickering behaviour (e.g. particle dimensions), adopting an active carrying/delivery functionality will not impede the particles' emulsion stabilisation performance.

3.2.3. *Encapsulation efficiency and loading capacity of lipid particles*

Previous work by the present authors on the characterisation of the particles' active carrying capability, revealed that changes to their chemical/physical properties do not alter their encapsulation efficiency (EE) or loading capacity (LC); with values of 99.9 ± 0.0% and 5.0 ± 0.0% for each of these, respectively [29]. Values within this range

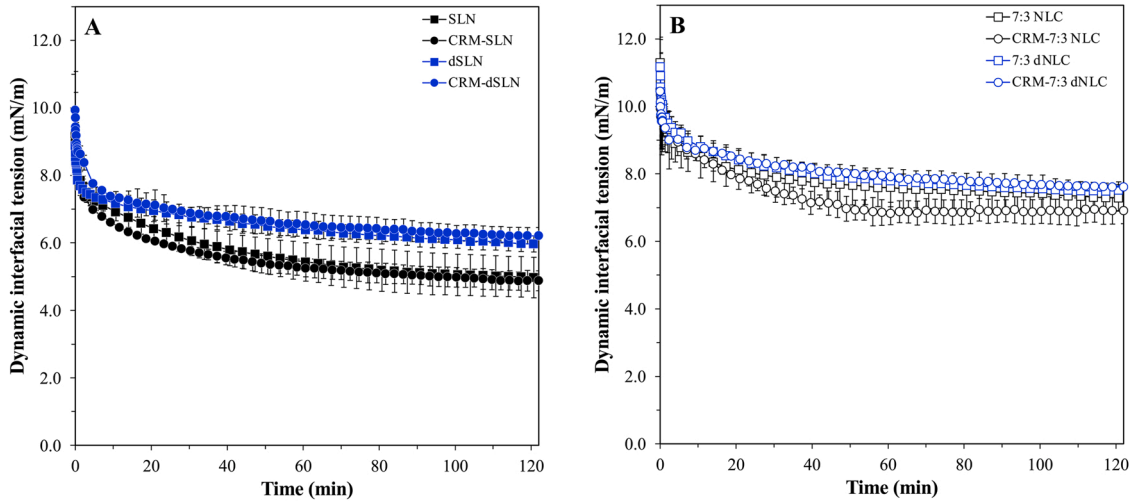

Fig. 6. Dynamic interfacial tension of aqueous dispersions of blank and CRM-loaded SLN (A) and 7:3 NLC formulations (B) used as produced and after dialysis. Data points are the average of three measurements and error bars represent the standard deviation.

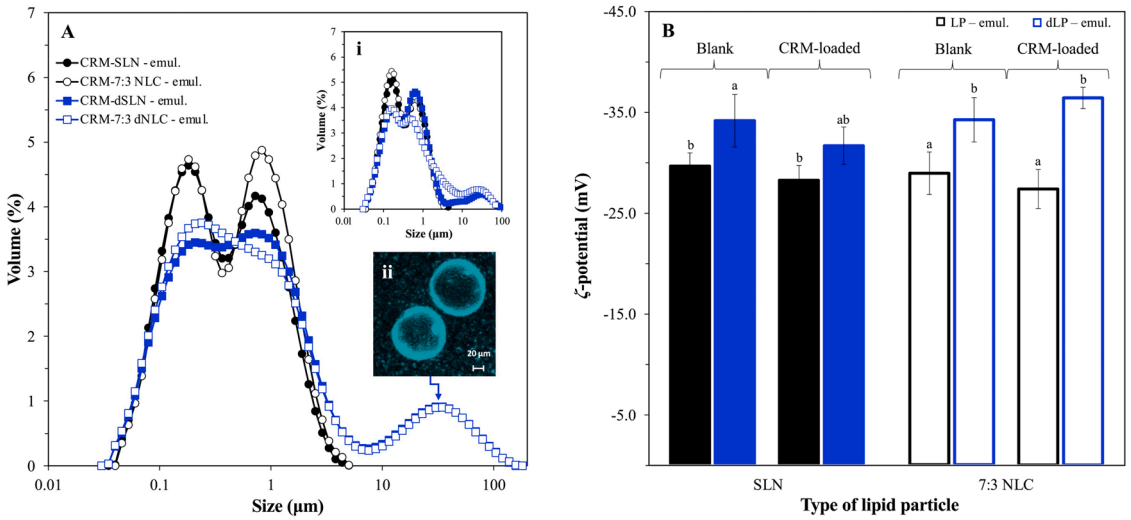

Fig. 7. Droplet size distribution (A) and ζ-potential (B) of o/w emulsion droplets stabilised with curcumin-loaded lipid particles used as produced (CRM-loaded LP) and after dialysis (CRM-loaded dLP). A CLSM image of selectively captured droplets of one of the systems is also depicted to illustrate the particle-covered interface (inset graph A, ii). The respective data for droplet size (inset graph A, i) and ζ-potential (B) for blank lipid particle-stabilised emulsions are also presented for comparison. Identical lowercase letters indicate no significant differences between samples (for $p < 0.05$ and sample size equal to 3).

have been previously reported for similar systems, where the incorporation of curcumin was achieved by simple solubilisation in lipid melts under stirring [45,46], whereas higher LC values were attained when organic solvents where employed [47,48]. Overall, the affinity of curcumin for the lipid matrix components (lipid and/or surfactant type and concentration) used was shown to greatly affect the obtained values. In the current study, the amount of curcumin persisting within the (as produced) SLNs and 7:3 NLCs following dialysis, after incorporation within an emulsion microstructure, but also over storage, was evaluated by measuring both the corresponding EE and LC values. Herein, the values determined for both parameters were the same as for the aqueous lipid particle dispersions. Notably, neither exposure of the particles to the dialysis conditions, nor introduction of a second phase (oil droplets) during emulsification, compromised their active carrying capacity. Thus, curcumin appears to maintain a close association with the microstructure, with no evidence of migration to the continuous phase. This could be possibly the result of the good solubilisation capacity/affinity of the used lipid matrix components for the active, as has been previously shown [29], but also a consequence of the relatively low quantity of active used/entrapped, allowing for an improved detainment within the colloidal microstructures. However, it should also be noted here, that within an emulsion setting, the absence of the active from the continuous aqueous phase does not necessarily confirm that the high encapsulation efficiencies are maintained due to the presence of the active solely within the particle structure. The prospect of a level of active migration to the oil used as the dispersed phase (i.e. the oil droplets that the particles are stabilising and thus are in partial contact with) is also possible. This is discussed in more detail in the following section.

3.2.4. *In vitro release performance of lipid particles*

The initial parts of this work have demonstrated the ability of the lipid particles (studied here) to successfully exhibit a Pickering functionality while also acting as active carriers. The present section investigates the parameters affecting the capacity of these lipid structures to deliver their encapsulated load. What is more, it also assesses how lipid particle placement within an emulsion setting (interface or continuous phase) impacts on the release performance demonstrated by the same colloidal species when present within a simple aqueous environment; i.e. release exhibited by the lipid particles in an aqueous dispersion. In both cases, the functionality of the lipid particles as delivery systems, was investigated prior and post dialysis. The SLN (Fig. 8*A*) and 7:3 NLC (Fig. 8*B*) lipid formulations, that were previously confirmed to be able to retain both functionalities of Pickering stabilisation and active carrying, were here employed to study the release of curcumin, selected as a model hydrophobic active [29].

It appears that both types of particles (in an aqueous dispersion) can function as release regulators for curcumin, with the obtained release rates showing drastic decrease compared to that from a pure curcumin aqueous solution; the latter having a curcumin concentration equivalent to that present in the continuous phase of both particles and emulsion systems, if none was contained within the dispersed phase. More specifically, the 7:3 NLCs demonstrated even more sustained release than the SLNs (both as undialysed lipid particles in dispersion), with 12.2% and 21.2% of curcumin released after 7 days, respectively. The differences in the curcumin release profiles cannot be explained in terms of particles size changes between the SLN (165 nm) and NLC (163 nm) lipid structures [29]. Instead, it could be that the incorporation of liquid lipid in the NLCs gives rise to structural re-organisation of the lipid particle matrix by the creation of a less ordered crystalline state, which could also be seen in their DSC profiles [29]. Such an effect could ultimately alter the active distribution/localisation within the particle structure, that could sequentially lead to acceleration [49,50] or hindering of the release profile [51]. Increase in the particles' liquid lipid content could also impact the relative compatibility between the active and the lipid matrix components, which (in this case) results in a hindrance of the release of the former [10,52]. Conversely, the dialysed particles (dSLNs and dNLCs) demonstrated an increased release rate compared to their undialysed equivalents. This could have been instigated by the exposure of particles (dSLNs and 7:3 dNLCs) to the dialysis conditions (e.g. high osmotic stress) and bulk aqueous environment (of equivalent capacity/volume to that used during the release experiments themselves) for longer periods of time than the undialysed ones.

In contrast, curcumin release from lipid particles within an emulsion setting (particles also acting as Pickering stabilisers for the emulsion droplets) was faster than that exhibited by equivalent particles in an aqueous dispersion (Fig. 8*A & B*). Similarly to what was observed earlier for the aqueous particle dispersions, emulsions fabricated with either dSLNs or 7:3 dNLCs (dialysed particles), showed a slightly higher release rate compared to their undialysed counterparts. Furthermore, when comparing the release profiles of the 7:3 NLC-stabilised emulsions to that of the respective SLN-stabilised systems, it is shown that the release

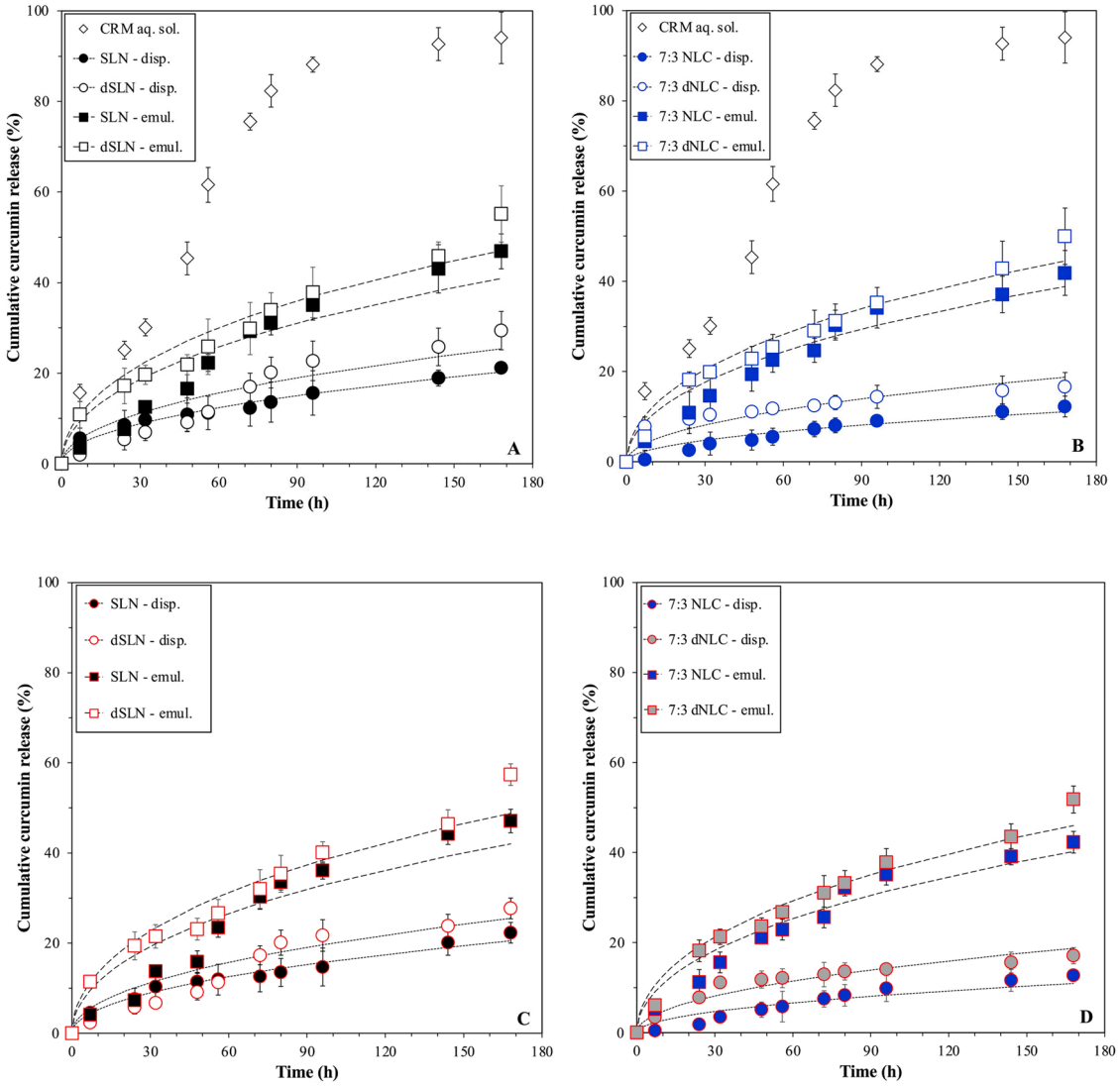

Fig. 8. *In vitro* release profile of a model hydrophobic active (curcumin) from SLN (A) and 7:3 NLC (B) dispersions used as produced and after dialysis, and also after emulsion incorporation. The release profile from a curcumin solution obtained under the same conditions is also depicted. The long-term stability of the release performance after 3 months of storage is depicted for all systems in (C) and (D), respectively. The in vitro release kinetic Crank model fitting of curcumin for each dispersion (dotted line) and emulsion system (dashed line) is also presented.

rate of the former was marginally slower. As such, these observations suggest that the presence on an oil phase (in the emulsion scenario) plays a crucial role in the discharge of curcumin. At the same time, the perpetuation of the particles' release performance (to a certain degree) indicates that the active regulation ability of each particle type persists even within an emulsion setting.

Fitting the curcumin release data to the Crank model [30] gave diffusion coefficient (*D*) values for the particles within the dispersion environment ranging between 9.96 and 719 $\times$ 10^{-20} cm^2 s^{-1}, while for those present in the emulsions the respective values were (in most instances) an order of magnitude higher (Table 2). The diffusion coefficients determined here for all systems are lower than the values reported in literature for curcumin-loaded SLNs fabricated with stearic acid as the lipid phase and Poloxamer 188 as surfactant [7,53]. The type of lipid source and surfactant used and their affinity for the enclosed active have been previously shown to influence the active loading capacity [29,46], which in turn can impact on the delivery performance. The lower *D* values reported here are in line with the high encapsulation efficiency/loading capacity values reported for all formulations, regardless of dialysis and/or emulsion presence. This is indicative of not only the close association of curcumin with the particles' crystalline

Table 2
Diffusion coefficient (D) and coefficient of determination (R^2) describing the fitting into the Crank model of the release data from lipid particles used as produced and after dialysis, and from particle-stabilised emulsions. For the emulsions, data fitting is performed on systems prepared with freshly produced and stored lipid particle dispersions (4 months), and for stored emulsion systems (3 months) prepared with fresh particle dispersions.

Formulation	Storage period (months)	$D \times 10^{-20}$ (cm^2 s^{-1})	R^2
SLN – disp.	0	45.1	0.98
dSLN – disp.	0	719	0.92
7:3 NLC – disp.	0	9.96	0.97
7:3 dNLC – disp.	0	11.9	0.93
SLN – emul.	0	212	0.94
	0 (stored particles)	216	0.91
	3	227	0.93
dSLN – emul.	0	311	0.96
	3	340	0.96
7:3 NLC – emul.	0	177	0.97
	0 (stored particles)	194	0.94
	3	192	0.97
7:3 dNLC – emul.	0	268	0.98
	3	290	0.99

matrix leading to slow diffusion, but also corroborative of the relatively low percentage of curcumin being released. Considering the above, along with the persistence of the EE values after addition of the particles within the emulsion setting, it could be proposed that the release of curcumin could only be ascribed to diffusion either from the free particles and/or from within the microstructure provided by the Pickering emulsions.

According to the data reported above, it is clear that the exposure of the particles to the oil phase creates circumstances that accelerate the release of curcumin into the aqueous acceptor phase. Delving further into the behaviour of the particles within the emulsion systems, a condition that could explain the effect of the emulsion addition, is the differentiation between the particles adsorbed at the oil-water interface and those remaining in the continuous phase. It is therefore suggested that the relative location/setting renders the particles to experience different surroundings, as shown in the schematic representation (Fig. 9). One surrounding resembles that of a dispersion setting (Fig. 9*B.2*(*i*)), where the particles are only exposed to the aqueous environment of the continuous phase, and the other consisting of a hybrid setting (Fig. 9*B.2*(*ii*)), where part of the particle structure is exposed to the oil phase and the other experiencing the continuous phase environment. In terms of the discharge from the latter, the underlying mechanism could be the outcome of a number of different contributions. Among these, introduction of the oil phase could cause migration of curcumin molecules adsorbed near the oil/particle contact points to the oil phase, which following that are more easily released to the continuous phase. Although, this could only constitute a small contribution, as the release behaviour appears to remain unchanged overtime (Fig. 8*C & D*), but also due to the minimal solubilisation capacity of sunflower oil for curcumin [54]. Thereby, the obtained release profiles appear to be the composite of the release from free particles that follow the release seen in simple dispersions, oil droplets that release curcumin a lot faster compared to the solid structure of the lipid particles, and lastly interfacially-adsorbed particles that would be expected to feed into both previous two patterns. Overall, the particle positioning at the oil/water interface results in a heterogeneous release pattern for curcumin and an utterly accelerated discharge in the emulsion's continuous phase (Fig. 9*B.3*), compared to the homogeneous release pattern of curcumin in the aqueous environment of the lipid particle dispersion (Fig. 9*A.2*).

Further to the curcumin migration presented above, other explanations could also lie in the creation of an added change-inducing potential to the particles themselves and around them, that leads to faster expulsion of curcumin. This could be stemming either from possible movement of the adsorbed surfactant molecules from the particle surface being in immediate exposure to the oil droplets [23,28,55], or even alterations to the arrangement of their hydrophilic chains, owing to changes in their surrounding environment [56,57]. Any of these explanations could lead to stripping of any loosely adsorbed curcumin near the particles' surface. Such phenomena appear to have further intensified in the dialysed particle-stabilised emulsions, causing slightly higher release rates and *D* values (Fig. 8*A & B,* Table 2). It was earlier shown (Fig. 3) that dialysed particles (dSLNs or dNLCs) have a higher interfacial presence, thus the faster release exhibited by their emulsions aligns well with the hypothesis presented here; i.e. that the presence of lipid particles at the emulsion interface facilitates further active discharge. The interaction and subsequent faster transfer of a fluorescent probe (25-NBD cholesterol) from adsorbed loaded-lipid particles to the oil phase compared to free loaded-particles in the continuous phase (and thus not directly associated with the emulsion droplets) could also be endorsed by the work of Schröder et al. [27]. Although minimal (as indicated by the DSC data presented earlier), the contribution of crystalline matter loss to the migration of the active from the particles to the oil phase (droplets) of the emulsion, should also be considered.

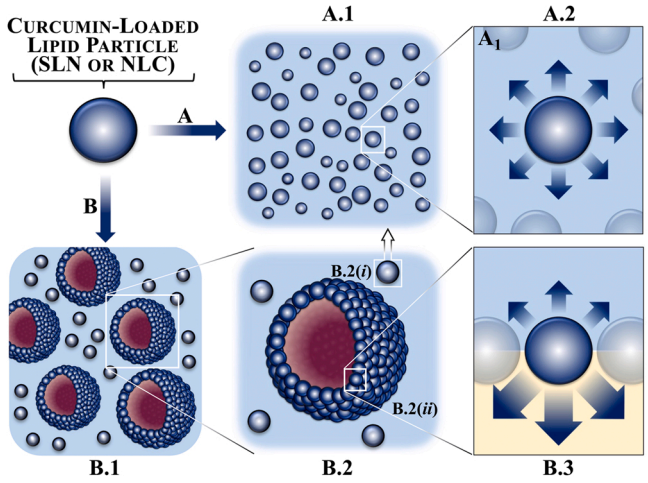

Fig. 9. Schematic diagram of the proposed release mechanism from lipid particles within aqueous dispersion (A) and emulsion (B) settings.

In an attempt to visualise the location of curcumin within the emulsion systems, the emulsion droplets were made larger (see *Section 2.7*) and CLSM was employed. Curcumin fluorescence [58] was primarily detected at the droplet interface and at particles remaining free in the continuous phase, of a representative emulsion system after 1 h of production (Fig. 10*A*). This implies the association of curcumin with the particles (in this case SLNs), whereas after 1 day of storage curcumin could be also identified within the oil droplets (Fig. 10*B*). However, this only stands as supportive evidence of the migration of a small proportion of curcumin in the oil phase (also owing to the low solubility in sunflower oil [54]), rather than a quantification approach, as due to the nature of the visualisation, any occurring events can appear exaggerated. A similar approach was taken in a study by Milsmann et al. [28], where CLSM was used to visualise the transfer of coumarin 6 from tristearin SLNs to the oil phase of MCT o/w emulsions (pre-stabilised with different surfactants). This phenomenon is proposed to take place within a short period of time after preparation, as already after 1 day a level of migration from the adsorbed particles to the droplets can be distinguished, although the quantity is expected to be small in comparison to the total amount that came into the emulsion system through the particles. The latter is further suggested by the lack of substantial loss of crystalline matter and the consistent release profiles obtained following long-term storage of both the lipid particle containing dispersions and emulsions (Fig. 8*C & D*). Further investigations in the previously reported work [28] using a separated model emulsion system (containing pseudo-phases) and electron paramagnetic resonance (EPR) spectroscopy revealed the role of surfactant micelles as facilitators of the lipophilic spin probe TEMPOL-benzoate (2,2,6,6-tetramethyl-4-piperidinol-1-oxyl benzoate, TB) transfer between the two phases. Additionally, it was proposed that the probe was primarily expelled from the surface of the particles, rather than the crystalline matrix. Herein, the presence of surfactant micelles both in the continuous phase (only in undialysed particle dispersions) and within the dissolution medium accommodated the curcumin transport towards the acceptor phase. The particle structural properties, particularly the composition of their surface layer, is an aspect that could greatly impact the release kinetics of actives either encapsulated within lipid particles in a dispersion environment, or particle-stabilised emulsion droplets. Formation of thick layers due to the presence of bulkier proteins around the particles which in turn occupy the interface [7], or capsule-like layers created by the partial melting of the lipid particles at the interface of the oil droplets [23], can result in hindered release rates. Thus, the role of the particles as either facilitators or inhibitors of the active passage from the crystalline structure that can halt the release rate, to the oil phase that can on the other hand accelerate it, could be manipulated by altering the interfacial properties of the former.

Lastly, the ability of the (curcumin-loaded) SLNs and NLCs to retain

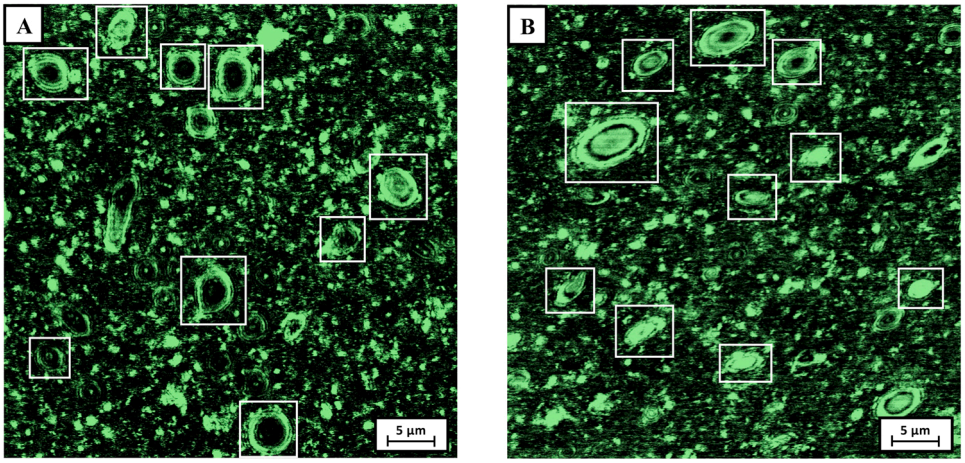

Fig. 10. Representative images of CRM-loaded SLN-stabilised o/w emulsions acquired using CLSM within 1 h after production (A) and after 1 d of storage (B), indicating the possibility of CRM migration from SLN to the oil droplets. White borders around droplets are used to indicate where the described phenomenon is more pronounced.

their release performance following prolonged storage was assessed. Curcumin release data were collected from either lipid particle-stabilised emulsions that were stored for up to 3 months (Fig. 8*C & D*), or from 'fresh' emulsions produced using particles that had been stored (as aqueous dispersions) for up to 4 months (Fig. S3). In both cases (and for both SLNs and NLCs), an almost identical release behaviour to that of 'freshly' produced emulsions stabilised by 'freshly' produced lipid particles, was exhibited (Fig. 11). The persistence of the particles' release behaviour even after 4 months of storage further highlights the catalytic effect of the oil phase (droplet) addition on the release rate observed from the emulsion systems. Similar data regarding prolonged storage release have been previously reported for bovine serum albumin (BSA) release from double-layer chitosan-based particles [59,60] and for telmisartan (hydrophobic drug) release from liquisolid compacts [59,60], although literature appears to be quite limited. For microstructures intended to be used as active carriers and delivery systems, this is a particularly important attribute, as it contributes to broadening their application prospect.

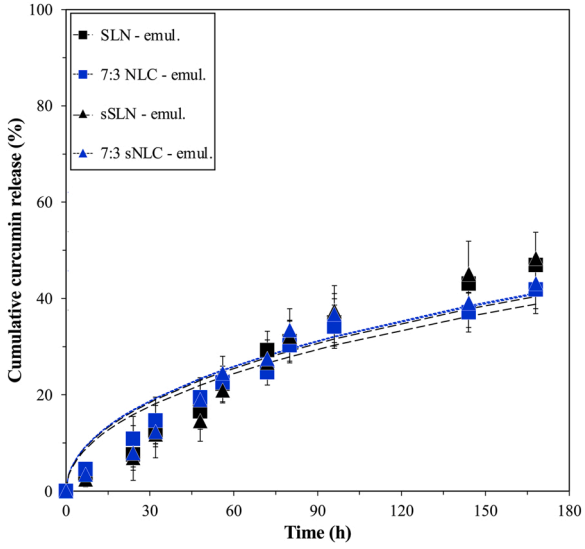

Fig. 11. Comparison of the in vitro release profile of curcumin from SLN and 7:3 NLC-stabilised emulsions fabricated with particles immediately after their preparation (SLN and 7:3 NLC), and after 4 months of storage (sSLN and 7:3 sNLC). *In vitro* release kinetic Crank model fitting of curcumin is presented with a dotted line for the former and a dashed line for the latter.

4. Conclusions

Having already established the Pickering functionality of both SLNs and NLCs used as produced and after removal of remnant surfactant from their aqueous carrier phase (in part I), this study demonstrated their concurrent capacity to act as active carriers/delivery systems of an encapsulated model hydrophobic active, thus rendering them dual-functional. In addition to investigating the active holding/delivery performance of these lipid structures prior- and post-emulsification, and the effect of certain formulation parameters on these characteristics, part of the focus was also placed on exploring whether this secondary functionality would compromise their previously established properties. Monitoring of crystalline matter loss from the lipid particles, a parameter that has thus far been closely associated with their Pickering functionality, but also consequently their active delivery regulation ability, revealed that the particles maintained their structural integrity within emulsions up to 12 weeks in storage conditions. Regarding their fate within the emulsion environment, it is suggested that the proportion of lipid particles residing at the emulsion interface can be influenced by the presence of excess surfactant in the aqueous phase. However, the percentage of adsorbed particles was shown to remain unaffected throughout the storage period, irrespectively of the presence/absence of excess surfactant. In terms of the effect of active incorporation on the interfacial properties and Pickering stabilisation capacity of the lipid particles, it was shown that encapsulation of curcumin within the SLN and 7:3 NLC formulations did not invoke any changes on either. Further to confirming the Pickering stabilisation capacity of the curcumin-loaded lipid particles, the concurrent functionality of acting as active carriers and release regulators was studied. More specifically, employing both SLNs and NLCs, the ability to regulate the release of curcumin was exhibited both in a dispersion system and within an emulsion setting; with the differentiation in the release mechanisms between the two systems being attributed to the diversity in the surroundings that the interfacially-adsorbed and unadsorbed particles are experiencing. Future work using these dual-functional colloidal species could explore the use of simple o/w emulsions for the co-release of multiple actives, while devising further approaches to tailor their release performance, such as altering formulation parameters of the lipid particles.

CRediT authorship contribution statement

Georgia I. Sakellari: Conceptualization, Methodology, Formal analysis, Investigation, Writing – original draft. **Ioanna Zafeiri:** Writing – review & editing. **Hannah Batchelor:** Supervision, Writing – review &

editing. **Fotis Spyropoulos:** Supervision, Writing – review & editing, Funding acquisition.

Declaration of Competing Interest

The authors declare that they have no known competing financial interests or personal relationships that could have appeared to influence the work reported in this paper.

Data availability

Data will be made available on request.

Acknowledgements

This work was supported by funding from the Biotechnology and Biological Sciences Research Council (BBSRC) through the Midlands Integrative Bioscience Doctoral Training Partnership (BB/M01116X/1).

Appendix A. Supplementary material

Supplementary data associated with this article can be found in the online version at doi:10.1016/j.colsurfa.2022.130787.

References

[1] P. Vega-Vásquez, N.S. Mosier, J. Irudayaraj, Nanoscale drug delivery systems: from medicine to agriculture, Front. Bioeng. Biotechnol. 8 (2020) 79, https://doi.org/10.3389/fbioe.2020.00079.
[2] S.A.A. Rizvi, A.M. Saleh, Applications of nanoparticle systems in drug delivery technology, Saudi Pharm. J. 26 (2018) 64–70, https://doi.org/10.1016/j.jsps.2017.10.012.
[3] H.K. Batchelor, J.F. Marriott, Formulations for children: problems and solutions, Br. J. Clin. Pharmacol. 79 (2015) 405–418, https://doi.org/10.1111/bcp.12268.
[4] X.W. Chen, X.Y. Ning, X.Q. Yang, Fabrication of novel hierarchical multicompartment highly stable triple emulsions for the segregation and protection of multiple cargos by spatial co-encapsulation, J. Agric. Food Chem. 67 (2019) 10904–10912, https://doi.org/10.1021/acs.jafc.9b03509.
[5] F. Spyropoulos, D. Kurukji, P. Taylor, I.T. Norton, Fabrication and utilization of bifunctional protein/polysaccharide coprecipitates for the independent codelivery of two model actives from simple oil-in-water emulsions, Langmuir 34 (2018) 3934–3948, https://doi.org/10.1021/acs.langmuir.7b04315.
[6] W. Wang, H. Song, J. Zhang, P. Li, C. Li, C. Wang, D. Kong, Q. Zhao, An injectable, thermosensitive and multicompartment hydrogel for simultaneous encapsulation and independent release of a drug cocktail as an effective combination therapy platform, J. Control. Release 203 (2015) 57–66, https://doi.org/10.1016/j.jconrel.2015.02.015.
[7] G.I. Sakellari, I. Zafeiri, A. Pawlik, D. Kurukji, P. Taylor, I.T. Norton, F. Spyropoulos, Independent co-delivery of model actives with different degrees of hydrophilicity from oil-in-water and water-in-oil emulsions stabilised by solid lipid particles via a Pickering mechanism: a-proof-of-principle study, J. Colloid Interface Sci. 587 (2021) 644–649, https://doi.org/10.1016/j.jcis.2020.11.021.
[8] F.Q. Hu, S.P. Jiang, Y.Z. Du, H. Yuan, Y.Q. Ye, S. Zeng, Preparation and characterization of stearic acid nanostructured lipid carriers by solvent diffusion method in an aqueous system, Colloids Surf. B Biointerfaces 45 (2005) 167–173, https://doi.org/10.1016/j.colsurfb.2005.08.005.
[9] L.J. Jia, D.R. Zhang, Z.Y. Li, F.F. Feng, Y.C. Wang, W.T. Dai, C.X. Duan, Q. Zhang, Preparation and characterization of silybin-loaded nanostructured lipid carriers, Drug Deliv. 17 (2010) 11–18, https://doi.org/10.3109/10717540903431586.
[10] K. Oehlke, D. Behsnilian, E. Mayer-Miebach, P.G. Weidler, R. Greiner, Edible solid lipid nanoparticles (SLN) as carrier system for antioxidants of different lipophilicity, PLoS One 12 (2017), e0171662, https://doi.org/10.1371/journal.pone.0171662.
[11] L. Becker Peres, L. Becker Peres, P.H.H. de Araújo, C. Sayer, Solid lipid nanoparticles for encapsulation of hydrophilic drugs by an organic solvent free double emulsion technique, Colloids Surf. B Biointerfaces 140 (2016) 317–323, https://doi.org/10.1016/j.colsurfb.2015.12.033.
[12] J. Weiss, E.A. Decker, D.J. McClements, K. Kristbergsson, T. Helgason, T. Awad, Solid lipid nanoparticles as delivery systems for bioactive food components, Food Biophys. 3 (2008) 146–154, https://doi.org/10.1007/s11483-008-9065-8.
[13] P. Jaiswal, B. Gidwani, A. Vyas, Nanostructured lipid carriers and their current application in targeted drug delivery, Artif. Cells Nanomed. Biotechnol. 44 (2016) 27–40, https://doi.org/10.3109/21691401.2014.909822.
[14] A. Borges, V. de Freitas, N. Mateus, I. Fernandes, J. Oliveira, Solid lipid nanoparticles as carriers of natural phenolic compounds, Antioxidants 9 (2020) 998, https://doi.org/10.3390/antiox9100998.
[15] E.B. Souto, S.A. Wissing, C.M. Barbosa, R.H. Müller, Development of a controlled release formulation based on SLN and NLC for topical clotrimazole delivery, Int. J. Pharm. 278 (2004) 71–77, https://doi.org/10.1016/j.ijpharm.2004.02.032.
[16] W. Mehnert, K. Mäder, Solid lipid nanoparticles: production, characterization and applications, Adv. Drug Deliv. Rev. 64 (2012) 83–101, https://doi.org/10.1016/j.addr.2012.09.021.
[17] S. Sapino, M.E. Carlotti, E. Pelizzetti, D. Vione, M. Trotta, L. Battaglia, Protective effect of SLNs encapsulation on the photodegradation and thermal degradation of retinyl palmitate introduced in hydroxyethylcellulose gel, J. Drug Deliv. Sci. Technol. 15 (2005) 159–165, https://doi.org/10.1016/s1773-2247(05)50021-2.
[18] E.B. Souto, R.H. Müller, SLN and NLC for topical delivery of ketoconazole, J. Microencapsul. 22 (2005) 501–510, https://doi.org/10.1080/02652040500162436.
[19] G.I. Sakellari, I. Zafeiri, H. Batchelor, F. Spyropoulos, Solid lipid nanoparticles and nanostructured lipid carriers of dual functionality at emulsion interfaces. Part I: Pickering stabilisation functionality, Colloids Surf. A Physicochem Eng. Asp. (2022), 130135, https://doi.org/10.1016/j.colsurfa.2022.130135.
[20] F. Spyropoulos, C. Clarke, D. Kurukji, I.T. Norton, P. Taylor, Emulsifiers of Pickering-like characteristics at fluid interfaces: Impact on oil-in-water emulsion stability and interfacial transfer rate kinetics for the release of a hydrophobic model active, Colloids Surf. A Physicochem Eng. Asp. 607 (2020), 125413, https://doi.org/10.1016/j.colsurfa.2020.125413.
[21] S. Frasch-Melnik, I.T. Norton, F. Spyropoulos, Fat-crystal stabilised w/o emulsions for controlled salt release, J. Food Eng. 98 (2010) 437–442, https://doi.org/10.1016/j.jfoodeng.2010.01.025.
[22] D.A. Garrec, S. Frasch-Melnik, J.V.L. Henry, F. Spyropoulos, I.T. Norton, Designing colloidal structures for micro and macro nutrient content and release in foods, Faraday Discuss. 158 (2012) 37–49, https://doi.org/10.1039/c2fd20024d.
[23] S.M. Dieng, N. Anton, P. Bouriat, O. Thioune, P.M. Sy, N. Massaddeq, S. Enharrar, M. Diarra, T. Vandamme, Pickering nano-emulsions stabilized by solid lipid nanoparticles as a temperature sensitive drug delivery system, Soft Matter 15 (2019) 8164–8174, https://doi.org/10.1039/c9sm01283d.
[24] I. Zafeiri, P. Smith, I.T. Norton, F. Spyropoulos, Fabrication, characterisation and stability of oil-in-water emulsions stabilised by solid lipid particles: the role of particle characteristics and emulsion microstructure upon Pickering functionality, Food Funct. 8 (2017) 2583–2591, https://doi.org/10.1039/c7fo00559h.
[25] I.T. Norton, C.D. Lee-Tuffnell, S. Ablett, S.M. Bociek, A calorimetric, NMR and X-ray diffraction study of the melting behavior of tripalmitin and tristearin and their mixing behavior with triolein, J. Am. Oil Chem. Soc. 62 (1985) 1237–1244, https://doi.org/10.1007/bf02541834.
[26] M. Samtlebe, U. Yucel, J. Weiss, J.N. Coupland, Stability of solid lipid nanoparticles in the presence of liquid oil emulsions, J. Am. Oil Chem. Soc. 89 (2012) 609–617, https://doi.org/10.1007/s11746-011-1944-3.
[27] A. Schröder, M. Laguerre, J. Sprakel, K. Schroën, C.C. Berton-Carabin, Pickering particles as interfacial reservoirs of antioxidants, J. Colloid Interface Sci. 575 (2020) 489–498, https://doi.org/10.1016/j.jcis.2020.04.069.
[28] J. Milsmann, K. Oehlke, R. Greiner, A. Steffen-Heins, Fate of edible solid lipid nanoparticles (SLN) in surfactant stabilized o/w emulsions. Part 2: release and partitioning behavior of lipophilic probes from SLN into different phases of o/w emulsions, Colloids Surf. A Physicochem Eng. Asp. 558 (2018) 623–631, https://doi.org/10.1016/j.colsurfa.2017.05.050.
[29] G.I. Sakellari, I. Zafeiri, H. Batchelor, F. Spyropoulos, Formulation design, production and characterisation of solid lipid nanoparticles (SLN) and nanostructured lipid carriers (NLC) for the encapsulation of a model hydrophobic active, Food Hydrocoll. Health (2021), 100024, https://doi.org/10.1016/j.fhfh.2021.100024.
[30] J. Crank. The Mathematics of Diffusion, second ed., Oxford University Press, London, 1975.
[31] J. Weiss, D.J. McClements, Mass transport phenomena in oil-in-water emulsions containing surfactant micelles: solubilization, Langmuir 16 (2000) 5879–5883, https://doi.org/10.1021/la9914763.
[32] D.J. McClements, S.R. Dungan, J.B. German, J.E. Kinsella, Evidence of oil exchange between oil-in-water emulsion droplets stabilized by milk proteins, J. Colloid Interface Sci. 156 (1993) 425–429, https://doi.org/10.1006/jcis.1993.1133.
[33] D.J. McClements, S.R. Dungan, J.B. German, J.E. Kinsella, Factors which affect oil exchange between oil-in-water emulsion droplets stabilized by whey protein isolate: protein concentration, droplet size and ethanol, Colloids Surf. A Physicochem Eng. Asp. 81 (1993) 203–210, https://doi.org/10.1016/0927-7757(93)80247-c.
[34] D.J. McClements, S.R. Dungan, Factors that affect the rate of oil exchange between oil-in-water emulsion droplets stabilized by a nonionic surfactant: droplet size, surfactant concentration, and ionic strength, J. Phys. Chem. 97 (2002) 7304–7308, https://doi.org/10.1021/j100130A030.
[35] A. Schröder, J. Sprakel, W. Boerkamp, K. Schroën, C.C. Berton-Carabin, Can we prevent lipid oxidation in emulsions by using fat-based Pickering particles? Food Res. Int. 120 (2019) 352–363, https://doi.org/10.1016/j.foodres.2019.03.004.
[36] A. Pawlik, D. Kurukji, I. Norton, F. Spyropoulos, Food-grade Pickering emulsions stabilised with solid lipid particles, Food Funct. 7 (2016) 2712–2721, https://doi.org/10.1039/c6fo00238b.
[37] O.O. Fasina, Z. Colley, Viscosity and specific heat of vegetable oils as a function of temperature: 35°C to 180°C, Int. J. Food Prop. 11 (2008) 738–746, https://doi.org/10.1080/10942910701586273.
[38] J.W.J. de Folter, E.M. Hutter, S.I.R. Castillo, K.E. Klop, A.P. Philipse, W.K. Kegel, Particle shape anisotropy in pickering emulsions: cubes and peanuts, Langmuir 30 (2014) 955–964, https://doi.org/10.1021/LA402427Q/SUPPL_FILE/LA402427Q_SI_002.AVI.

[39] W. Li, T. Suzuki, H. Minami, The interface adsorption behavior in a Pickering emulsion stabilized by cylindrical polystyrene particles, J. Colloid Interface Sci. 552 (2019) 230–235, https://doi.org/10.1016/j.jcis.2019.05.058.
[40] D.J. French, A.T. Brown, A.B. Schofield, J. Fowler, P. Taylor, P.S. Clegg, The secret life of Pickering emulsions: particle exchange revealed using two colours of particle, 6, Sci. Rep. 2016 6 (1) (2016) 1–9, https://doi.org/10.1038/srep31401.
[41] A. Schröder, J. Sprakel, K. Schroën, C.C. Berton-Carabin, Tailored microstructure of colloidal lipid particles for Pickering emulsions with tunable properties, Soft Matter 13 (2017) 3190–3198, https://doi.org/10.1039/c6sm02432g.
[42] M. Graca, J.H.H. Bongaerts, J.R. Stokes, S. Granick, Friction and adsorption of aqueous polyoxyethylene (Tween) surfactants at hydrophobic surfaces, J. Colloid Interface Sci. 315 (2007) 662–670, https://doi.org/10.1016/j.jcis.2007.06.057.
[43] X. Li, H. Li, Q. Xiao, L. Wang, M. Wang, X. Lu, P. York, S. Shi, J. Zhang, Two-way effects of surfactants on Pickering emulsions stabilized by the self-assembled microcrystals of a-cyclodextrin and oil, Phys. Chem. Chem. Phys. 16 (2014) 14059, https://doi.org/10.1039/c4cp00807c.
[44] P.Y. Liu, R.Y. Yang, A.B. Yu, Self-diffusion of wet particles in rotating drums, Phys. Fluids 25 (2013), 063301, https://doi.org/10.1063/1.4807596.
[45] V.H.S. Araujo, P.B. da Silva, I.O. Szlachetka, S.W. da Silva, B. Fonseca-Santos, M. Chorilli, R. Ganassin, G.R.T. de Oliveira, M.C.O. da Rocha, R.P. Fernandes, M. de Carvalho Vieira Queiroz, R.B. Azevedo, L.A. Muehlmann, The influence of NLC composition on curcumin loading under a physicochemical perspective and in vitro evaluation, Colloids Surf. A Physicochem Eng. Asp. 602 (2020), 125070, https://doi.org/10.1016/j.colsurfa.2020.125070.
[46] M.A. Espinosa-Olivares, N.L. Delgado-Buenrostro, Y.I. Chirino, M.A. Trejo-Márquez, S. Pascual-Bustamante, A. Ganem-Rondero, Nanostructured lipid carriers loaded with curcuminoids: physicochemical characterization, in vitro release, ex vivo skin penetration, stability and antioxidant activity, Eur. J. Pharm. Sci. 155 (2020), 105533, https://doi.org/10.1016/j.ejps.2020.105533.
[47] M.L. Bondì, M.R. Emma, C. Botto, G. Augello, A. Azzolina, F. di Gaudio, E. F. Craparo, G. Cavallaro, D. Bachvarov, M. Cervello, Biocompatible lipid nanoparticles as carriers to improve curcumin efficacy in ovarian cancer treatment, J. Agric. Food Chem. 65 (2017) 1342–1352, https://doi.org/10.1021/acs.jafc.6b04409.
[48] W. Wang, T. Chen, H. Xu, B. Ren, X. Cheng, R. Qi, H. Liu, Y. Wang, L. Yan, S. Chen, Q. Yang, C. Chen, Curcumin-loaded solid lipid nanoparticles enhanced anticancer efficiency in breast cancer, Molecules 23 (2018) 1578, https://doi.org/10.3390/molecules23071578.
[49] A. zur Mühlen, C. Schwarz, W. Mehnert, Solid lipid nanoparticles (SLN) for controlled drug delivery - drug release and release mechanism, Eur. J. Pharm. Biopharm. 45 (1998) 149–155, https://doi.org/10.1016/s0939-6411(97)00150-1.
[50] J. Liu, J. Zhu, Z. Du, B. Qin, Preparation and pharmacokinetic evaluation of Tashinone IIA solid lipid nanoparticles, Drug Dev. Ind. Pharm. 31 (2005) 551–556, https://doi.org/10.1080/03639040500214761.
[51] P.R. Ravi, N. Aditya, H. Kathuria, S. Malekar, R. Vats, Lipid nanoparticles for oral delivery of raloxifene: optimization, stability, in vivo evaluation and uptake mechanism, Eur. J. Pharm. Biopharm. 87 (2014) 114–124, https://doi.org/10.1016/j.ejpb.2013.12.015.
[52] G. Zoubari, S. Staufenbiel, P. Volz, U. Alexiev, R. Bodmeier, Effect of drug solubility and lipid carrier on drug release from lipid nanoparticles for dermal delivery, Eur. J. Pharm. Biopharm. 110 (2017) 39–46, https://doi.org/10.1016/j.ejpb.2016.10.021.
[53] W. Tiyaboonchai, W. Tungpradit, P. Plianbangchang, Formulation and characterization of curcuminoids loaded solid lipid nanoparticles, Int. J. Pharm. 337 (2007) 299–306, https://doi.org/10.1016/j.ijpharm.2006.12.043.
[54] P. Ma, Q. Zeng, K. Tai, X. He, Y. Yao, X. Hong, F. Yuan, Development of stable curcumin nanoemulsions: effects of emulsifier type and surfactant-to-oil ratios, J. Food Sci. Technol. 55 (2018) 3485–3497, https://doi.org/10.1007/s13197-018-3273-0.
[55] J. Milsmann, K. Oehlke, K. Schrader, R. Greiner, A. Steffen-Heins, Fate of edible solid lipid nanoparticles (SLN) in surfactant stabilized o/w emulsions. Part 1: interplay of SLN and oil droplets, Colloids Surf. A Physicochem Eng. Asp. 558 (2018) 615–622, https://doi.org/10.1016/j.colsurfa.2017.05.073.
[56] K. Szymczyk, A. Zdziennicka, B. Jańczuk, Effect of polysorbates on solids wettability and their adsorption properties, Colloids Interfaces 2 (2018) 26, https://doi.org/10.3390/colloids2030026.
[57] A. Amani, P. York, H. de Waard, J. Anwar, Molecular dynamics simulation of a polysorbate 80 micelle in water, Soft Matter 7 (2011) 2900–2908, https://doi.org/10.1039/c0sm00965b.
[58] M.A. Gogoleva, B.P. Yakimov, S.A. Rodionov, T.N. Tikhonova, Y.I. Gurfinkel, V. v. Fadeev, J. Lademann, M.E. Darvin, E.A. Shirshin, Solid lipid curcumin-loaded particles for in vivo fluorescent imaging in humans: a proof of concept, Opt. Spectrosc. 126 (2019) 730–735, https://doi.org/10.1134/s0030400×19060067.
[59] T. Xiang, J. Yang, S. Li, J. Li, W. Situ, Improvement in bioactive protein storage stability and colon-targeted release: a simple double-layer chitosan-based particle, J. Microencapsul. 36 (2019) 474–484, https://doi.org/10.1080/02652048.2019.1646336.
[60] N. Chella, N. Narra, T.R. Rao, Preparation and characterization of liquisolid compacts for improved dissolution of telmisartan, J. Drug Deliv. 2014 (2014) 1–10, https://doi.org/10.1155/2014/692793.